Dyakonov-Perel electron spin relaxation in a wurtzite semiconductor: From the nondegenerate to the highly degenerate regime

J. H. Buß,[1] J. Rudolph,[1] S. Starosielec,[1] A. Schaefer,[1] F. Semond,[2] Y. Cordier,[2] A. D. Wieck,[3] and D. Hägele[1]

[1]*Arbeitsgruppe Spektroskopie der kondensierten Materie, Ruhr-Universität Bochum, Universitätsstraße 150, D-44780 Bochum, Germany*

[2]*Centre de Recherche sur l'Hétéro-Epitaxie et ses Applications, Centre National de la Recherche Scientifique, Rue Bernard Gregory, Sophia Antipolis, F-06560 Valbonne, France*

[3]*Angewandte Festkörperphysik, Ruhr-Universität Bochum, Universitätsstraße 150, D-44780 Bochum, Germany*

(Received 18 November 2010; published 4 October 2011)

Electron spin lifetimes are investigated in bulk wurtzite n-GaN up to very high doping densities by time-resolved Kerr-rotation spectroscopy. The doping densities range from 5×10^{15} to 1.5×10^{19} cm^{-3}, corresponding to Fermi temperatures as high as 1200 K. The spin lifetime shows a maximum at the onset of degeneracy. The additional determination of momentum scattering times allows for a direct comparison with an analytical expression of the spin relaxation tensor in wurtzite semiconductors for a degenerate electron gas following Dyakonov-Perel theory. We find good agreement with the experiment up to the highest densities without any fitting parameter. The only known theoretical value $\alpha_e = 9.0$ meV Å of the k-linear contribution to spin-orbit coupling in the conduction band is shown to be valid up to the highest doping densities.

DOI: 10.1103/PhysRevB.84.153202 PACS number(s): 72.25.Rb, 78.47.D−, 78.66.Fd

Formulated in 1972, Dyakonov-Perel (DP) theory of spin relaxation in semiconductors has proved to be very successful in explaining electron spin relaxation from moderate to very high temperatures.[1] The main ingredients of DP theory are the momentum-dependent spin splitting caused by spin-orbit coupling (SOC) and a motional narrowing effect that reduces spin relaxation for faster carrier scattering. The spin splitting causes a k-dependent (momentum-dependent) precession of electrons spins around an effective magnetic field $\mathbf{\Omega}(\mathbf{k})$ and consequently initiates spin relaxation for a distribution of electrons in k space. Determination of the spin-relaxation tensor allows for probing the strength and symmetry of SOC[2] and for comparison with predictions from, e.g., kp, or tight-binding theory. Previously, the doping-dependent Dyakonov-Perel spin relaxation had been studied in zincblende semiconductors such as n-GaAs (Refs. 3–5) and n-CdTe (Ref. 6). There, a decrease of spin lifetimes with increasing degeneracy of the electron gas was found after a maximum at the onset of degeneracy. Jiang and Wu showed theoretically that this nonmonotonic density dependence is a universal behavior in zincblende III–V semiconductors in the metallic regime, which exists also in strained GaAs, where the SOC is dominated by a k-linear term.[3] Accordingly, a nonmonotonic density dependence of spin relaxation can also be expected for semiconductors with wurtzite structure,[7] where a k-linear term due to the wurtzite structure inversion asymmetry (WSIA) contributes to the SOC.

After the early work of Beschoten *et al.*,[8] the wide-gap semiconductor GaN in its wurtzite phase has shifted into the focus of interest for possible applications in spintronic and spin-optoelectronic devices. Beschoten *et al.* studied electron spin relaxation in three bulk GaN samples with doping densities from $n_D = 3.5 \times 10^{16}$ cm^{-3} to 9×10^{17} cm^{-3} and found the longest spin lifetime for the intermediate doping level.[8] Recently, anisotropic spin relaxation[9] and its temperature dependence were studied in moderately n-doped GaN up to 300 K.[10] Spin relaxation was found to be completely dominated by the intrinsic k-linear WSIA spin-orbit contribution via the Dyakonov-Perel mechanism. However, systematic experimental investigations up to the highest doping densities and theoretical treatment of DP spin relaxation in the degenerate wurtzite case have been missing so far. Here we investigate spin relaxation in 11 different bulk GaN samples with doping densities up to 1.5×10^{19} cm^{-3}, corresponding to Fermi temperatures up to 1200 K employing time-resolved Kerr-rotation (TRKR) spectroscopy. These measurements greatly exceed the densities investigated so far and therefore cover high k values of the carriers that had not been accessed before. We find a nonmonotonic density dependence of spin lifetimes and demonstrate a shift of the maximum of the spin lifetime toward higher densities for increasing lattice temperature. The reduction of spin lifetimes after the onset of degeneracy is much less dramatic than in the case of zincblende semiconductors. In addition, we derive an analytical expression for the density-dependent spin relaxation tensor for wurtzite semiconductors in the degenerate regime following Dyakonov-Perel theory. The additional determination of momentum scattering times allows a direct comparison to the experiment without any fitting parameter. Quantitative agreement is found up to the highest densities.

All 11 GaN samples investigated were grown by molecular beam epitaxy. Samples A1–A6, B, C1, C2, and E were grown on Si(111) substrate,[11] with the layer sequence given in Table I. Sample D consists of a 1 μm-thick n-type GaN layer on top of a 350-nm-wide GaN buffer layer, deposited on a GaN template.[12] The top GaN layer is n-doped with Si in each sample with a room-temperature doping level n_D determined by capacitance-voltage spectroscopy and secondary ion mass spectrometry (SIMS), respectively (sample A1: n_D (cm^{-3}) = 5×10^{15}, A2: 1.9×10^{17}, A3: 2.7×10^{17}, A4: 1.25×10^{18}, A5: 1.7×10^{18}, A6: 2.4×10^{18}, B: 4.5×10^{18}, C1: 6×10^{18}, C2: 1×10^{19}, D: 1×10^{19}, and E: 1.5×10^{19}).

The TRKR transients were measured with the setup described in Ref. 13. The energy of pump and probe pulse was varied between 3.458 eV for the lowest doped sample

TABLE I. Layer structure of samples A1–A6, B, C1, C2, and E, with layer thicknesses given in nm. Sample D is described in the text.

Sample A *(B)*		Sample C1 *(C2)*		Sample E	
Layer	Thickness	Layer	Thickness	Layer	Thickness
		n-GaN	236 *(194)*		
		GaN	295 *(291)*		
		p-GaN	492 *(485)*	*n*-GaN	194
n-GaN	2000 *(500)*	GaN	302 *(288)*	GaN	485
(GaN)[a]	*(1000)*	*n*-GaN	242 *(192)*	*n*-GaN	192
AlN	250	AlN	114 *(136)*	AlN	136
GaN	250	GaN	364 *(240)*	GaN	240
AlN	44	AlN	40 *(39)*	AlN	39
Si(111) substrate		Si(111) substrate		Si(111) substrate	

[a]An extra GaN layer is only in Sample B.

and 3.478 eV for the highest doping level at $T = 80$ K and between 3.404 and 3.411 eV at $T = 293$ K. The estimated density of photoexcited carriers was $n_{\text{exc}} = 2 \times 10^{15}$ cm^{-3} at $T = 80$ K and 2.8×10^{16} cm^{-3} at $T = 293$ K, respectively.[14] The samples were mounted in a cold-finger cryostat. An external magnetic field B_{ext} was applied in the sample plane.

Figure 1(a) shows TRKR transients for samples with a doping density n_D from 5×10^{15} up to 1×10^{19} cm^{-3} in a magnetic field $B_{\text{ext}} = 0.62$ T at $T = 80$ K. The transients show oscillations with frequency $\omega_L = g\mu_B B_{\text{ext}}/\hbar$ due to Larmor precession of the electron spins in an external magnetic field. The temporal decay of the transients directly reflects the spin relaxation. The corresponding spin relaxation time τ_s was extracted from exponential decay fits[15] $[A_1 \exp(-t/\tau_c) + A_2] \exp(-t/\tau_s)$ to the zero-field transients and damped-cosine fits $[A_1 \exp(-t/\tau_c) + A_2] \exp(-t/\tau_{s,B}) \cos[\omega_L(t - t_0)]$ to the transients for $B_{\text{ext}} > 0$, respectively.[16]

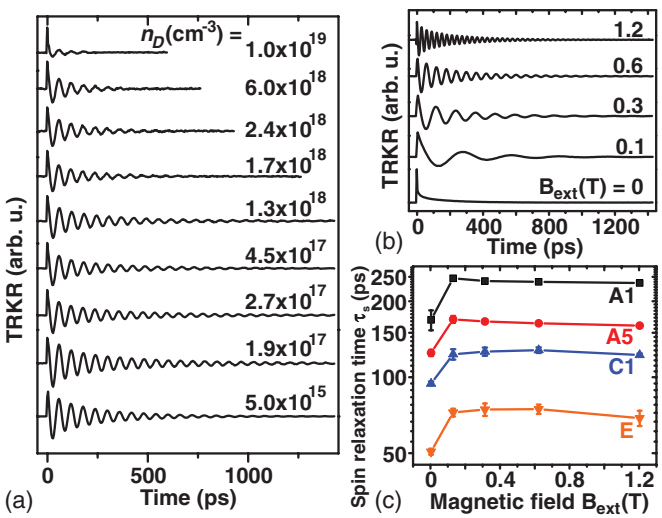

FIG. 1. (Color online) (a) TRKR transients for doping densities from $n_D = 5 \times 10^{15}$ to 1×10^{19} cm^{-3} at $T = 80$ K and in an external magnetic field of $B_{\text{ext}} = 0.62$ T. (b) TRKR transients for sample A1 ($n_D = 5 \times 10^{15}$ cm^{-3}) in magnetic fields $B_{\text{ext}} = 0$ T up to 1.2 T at $T = 80$ K. (c) Magnetic field dependence of the spin relaxation time τ_s for samples A1 ($n_D = 5 \times 10^{15}$ cm^{-3}), A5 ($n_D = 1.7 \times 10^{18}$ cm^{-3}), C1 ($n_D = 6.0 \times 10^{18}$ cm^{-3}), and E ($n_D = 1.5 \times 10^{19}$ cm^{-3}) at $T = 80$ K.

First, we will discuss the magnetic field dependence of spin relaxation. Figure 1(b) shows exemplarily TRKR transients for different external magnetic fields B_{ext} for sample A1. The magnetic field dependence of the corresponding spin relaxation time is shown in Fig. 1(c) for samples A1, A5, C1, and E with doping densities from $n_D = 5 \times 10^{15}$ cm^{-3} to $n_D = 1 \times 10^{19}$ cm^{-3}. The sudden increase of the spin relaxation time from its zero-field value τ_s to $\tau_{s,B} = 4/3\tau_s$ in an external magnetic field is a consequence of the intrinsic spin relaxation anisotropy in wurtzite semiconductors, as elaborated in Ref. 9. The anisotropy clearly persists up to the highest investigated doping level.

As the central result, the doping density dependence of spin relaxation is shown in Fig. 2 for $T = 80$ K and $T = 293$ K, where the zero-field values $\tau_s(n_D)$ (solid symbols) and the values $3/4\overline{\tau_{s,B}}(n_D)$ (open symbols) averaged over the spin relaxation times $\tau_{s,B}$ at finite magnetic fields[10] are plotted. A nonmonotonic density dependence of spin relaxation is observed at both temperatures, with a shift of the maximum spin lifetime to higher densities for increasing lattice temperature.

In the following, we will show that this nonmonotonic density dependence can be well explained by Dyakonov-Perel relaxation, similar to the theoretical description for zincblende semiconductors by Jiang and Wu.[3] The intrinsic conduction-band spin splitting is described by the Dresselhaus and the WSIA contribution,[17] combined in the Hamiltonian[10,18] $H_{so} = H_{so}^D + H_{so}^W = \frac{\hbar}{2}\boldsymbol{\Omega}(\mathbf{k}) \cdot \boldsymbol{\sigma}$, with the effective magnetic field $\boldsymbol{\Omega}(\mathbf{k})$ and the vector of Pauli spin matrices $\boldsymbol{\sigma}$. The tensor γ_{ij} of spin relaxation rates is obtained by[19]

$$\gamma_{ij} = \tfrac{1}{2}(\delta_{ij}\langle\boldsymbol{\Omega}^2\rangle - \langle\Omega_i\Omega_j\rangle)\tau_p \,, \qquad (1)$$

where $i, j = x, y, z$, $\langle\cdots\rangle$ denotes averaging over the electrons' momentum distribution, and τ_p is the momentum scattering time. The density dependence of the corresponding spin relaxation time is therefore determined by both the effective magnetic field average $\langle\Omega_{\text{eff}}^2\rangle \equiv \frac{1}{2}\left(\delta_{ij}\langle\boldsymbol{\Omega}^2\rangle - \langle\Omega_i\Omega_j\rangle\right)$ and the momentum scattering time τ_p. Two regimes can be distinguished by the ratio T/T_F of lattice temperature T to the Fermi temperature $T_F = E_F/k_B$, which is

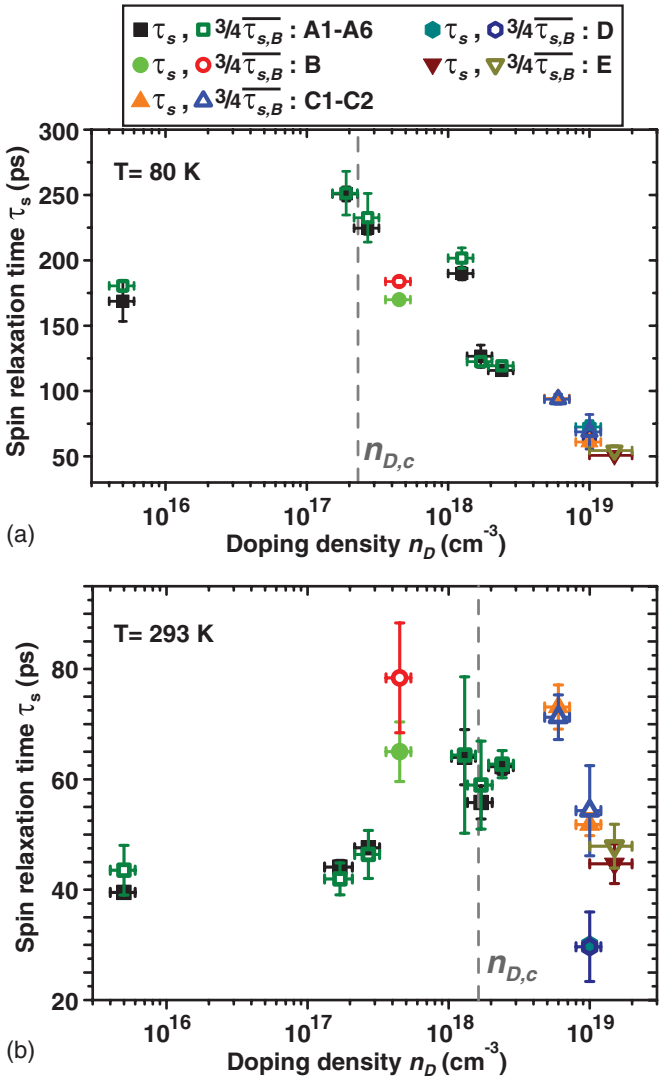

FIG. 2. (Color online) Doping density dependence of the spin relaxation time τ_s at (a) $T = 80$ K and (b) $T = 293$ K. The dashed line indicates the critical density $n_{D,c}$ (see text).

determined by the electron density n_D via the Fermi energy $E_F = (3\pi^2)^{2/3}\hbar^2 n_D^{2/3}/2m^*$.

(i) In the *non-degenerate regime*, the Fermi temperature is below the lattice temperature, $T_F \ll T$, and $\langle\Omega_{\rm eff}^2\rangle$ varies only weakly with density. The momentum scattering is dominated by electron-impurity scattering and electron-electron scattering,[20] with corresponding momentum scattering times $\tau_p^{ei} \propto n_D^{-1}$ and $\tau_p^{ee} \propto n_D^{-1}$, respectively, which decrease with increasing density in the nondegenerate regime.[3,7,21] The spin relaxation time τ_s increases therefore with increasing density. (ii) In the *degenerate regime*, the Fermi temperature is above the lattice temperature, $T_F \gg T$, and momentum scattering is dominated by electron-impurity scattering, which is approximately independent of the density for a degenerate electron gas ($\tau_p^{ei} \propto$ const).[7,22] The spin relaxation time then decreases with increasing density since $\langle\Omega_{\rm eff}^2\rangle$ increases with density in the degenerate regime due to the occupation of higher k states. In total, a nonmonotonic density dependence of spin relaxation results, with maximum spin lifetimes in the crossover regime at a critical density $n_{D,c}$, for which the Fermi temperature $T_F(n_{D,c}) \approx T$ is comparable to the lattice temperature T. Accordingly, a shift of $n_{D,c}$ toward higher densities is expected for increasing lattice temperature T. This shift can be clearly seen by comparing the density-dependent spin lifetimes at $T = 80$ K and $T = 293$ K in Fig. 2. The experimental densities for maximum spin lifetimes agree also very well with the calculated values of $n_{D,c} = 2.3 \times 10^{17}$ cm^{-3} for $T_F = T = 80$ K and $n_{D,c} = 1.6 \times 10^{18}$ cm^{-3} for $T_F = T = 293$ K (see dashed lines in Fig. 2).[23]

Finally, we discuss the density dependence of spin relaxation in the highly degenerate regime. The spin relaxation tensor in the degenerate regime can be calculated from Eq. (1) with the effective magnetic field[7,10,18]

$$\Omega(\mathbf{k}) = \frac{2}{\hbar}\begin{pmatrix} \left[\gamma_e\left(bk_z^2 - k_\parallel^2\right) + \alpha_e\right]k_y \\ -\left[\gamma_e\left(bk_z^2 - k_\parallel^2\right) + \alpha_e\right]k_x \\ 0 \end{pmatrix}, \qquad (2)$$

where $z\|[0001]$ (c axis), $x\|[11\bar{2}0]$, $y\|[1\bar{1}00]$, and $k_\parallel^2 = k_x^2 + k_y^2$. The parameters γ_e and b determine the strength of the Dresselhaus contribution, while α_e gives the size of the WSIA contribution. The spin relaxation time

$$\tau_s^W = \frac{1}{\gamma_{zz}^W} = \frac{3^{1/3}\hbar^2}{4\pi^{4/3}\alpha_e^2}\frac{1}{n_D^{2/3}}\frac{1}{\tau_p} \qquad (3)$$

due to only the WSIA contribution follows from Eq. (1) by averaging over the angular distribution of $\mathbf{k}$ and replacing k by the Fermi wave vector $k_F^2 = (3\pi^2)^{2/3} n_D^{2/3}$, which is a good approximation in the degenerate regime. The spin relaxation time

$$\tau_s^D = \frac{1}{\gamma_{zz}^D} = \frac{35\hbar^2}{12(3b^2 - 8b + 24)\pi^4\gamma_e^2}\frac{1}{n_D^2}\frac{1}{\tau_p} \qquad (4)$$

due to only the Dresselhaus contribution follows analogously[24] and exhibits the steep $\tau_s^D \propto n_D^{-2}$ dependence well known from zincblende semiconductors. We note that the intrinsic spin

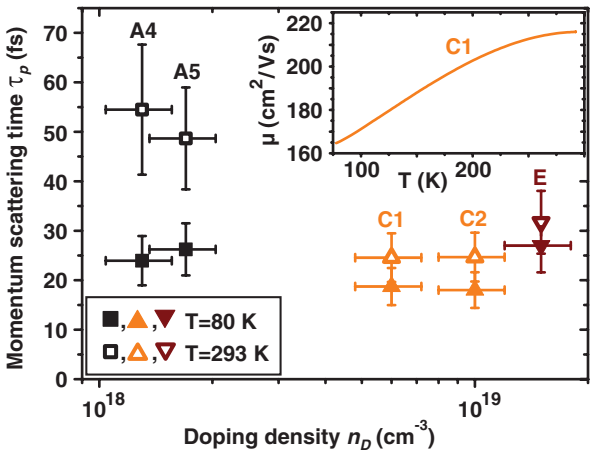

FIG. 3. (Color online) Doping density dependence of the momentum scattering time τ_p in the degenerate regime $n_D \geqslant 1.3 \times 10^{18}$ cm^{-3} as determined by van der Pauw measurements at $T = 80$ K (solid symbols) and $T = 293$ K (open symbols). The inset shows the temperature dependence of the mobility μ exemplarily for sample C1.

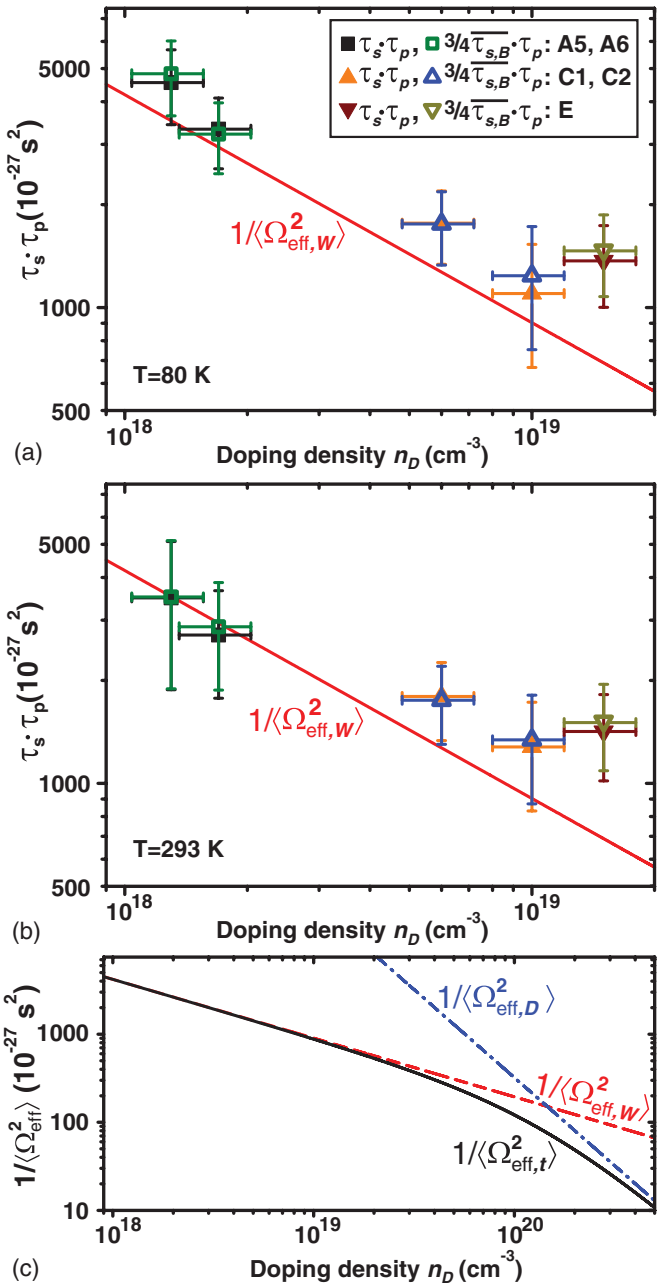

FIG. 4. (Color online) Doping density dependence of the product $\tau_s\tau_p$ of spin relaxation time and momentum scattering time at (a) $T = 80$ K and (b) $T = 293$ K. The solid line shows the inverse averaged effective magnetic field $1/\langle\Omega^2_{\mathrm{eff,W}}\rangle$ calculated according to Eq. (5) for only the WSIA contribution. (c) Calculated doping density dependence of the inverse effective magnetic field $1/\langle\Omega^2_{\mathrm{eff,W}}\rangle$ for only the WSIA contribution (dashed line), $1/\langle\Omega^2_{\mathrm{eff,D}}\rangle$ for only the Dresselhaus contribution (dashed-dotted line), and $1/\langle\Omega^2_{\mathrm{eff,t}}\rangle$ for both contributions simultaneously (solid line).

relaxation anisotropy[9] with $\gamma_{zz} = 2\gamma_{xx} = 2\gamma_{yy}$ persists, which implies that the above expression for $\mathbf{\Omega}(\mathbf{k})$ is consistent with our experimental findings up to very high k values.

We further determined the momentum scattering time τ_p by van der Pauw measurements for $n_D \geqslant 1.3 \times 10^{18}$ cm^{-3} to compare the spin relaxation times predicted by Eqs. (3) and (4) with the experimental results.[25] Figure 3 shows the corresponding values for τ_p at $T = 80$ K (solid symbols) and $T = 293$ K (open symbols). The inset shows the typical temperature dependence of the mobility μ exemplarily for sample C1.[26]

The purely experimentally determined product $\tau_s\tau_p$ can then be compared to the calculated averaged effective magnetic field $\langle\Omega^2_{\mathrm{eff}}\rangle$, based on the relation $\tau_s\tau_p = 1/\langle\Omega^2_{\mathrm{eff}}\rangle$ following from Eq. (1). Figure 4 shows very good agreement between the experimental values and the effective magnetic field

$$\langle\Omega^2_{\mathrm{eff,W}}\rangle = \frac{4\pi^{4/3}\alpha_e^2}{3^{1/3}\hbar^2} n_D^{2/3} \tag{5}$$

due to only the WSIA contribution, where the only material parameter entering is $\alpha_e = 9.0$ meV Å as obtained by tight-binding calculations.[18,27] The spin relaxation time τ_s shows therefore clearly a $\tau_s \propto n_D^{-2/3}$ density dependence, demonstrating that the WSIA contribution dominates DP spin relaxation in GaN even up to doping densities of 1.5×10^{19} cm^{-3}. This $\tau_s \propto n_D^{-2/3}$ density dependence is distinctively different from the $\tau_s \propto n_D^{-2}$ behavior observed in zincblende semiconductors. The domination of the WSIA contribution is in agreement with the only available parameter set $\alpha_e = 9.0$ meV Å, $\gamma_e = 0.32$ eV Å^3, and $b = 3.959$,[18,27] for which the Dresselhaus contribution is expected to dominate DP spin relaxation only for very high densities $n_D > 10^{20}$ cm^{-3} [see Fig. 4(c)].

Equation (2) is derived within kp theory by an expansion in the wave vector k around the Γ point ($k = 0$). The kp model breaks down for large wave vectors,[28] as is well known from, e.g., full-zone calculations of the spin splitting in zincblende semiconductors.[29] Here the very good agreement of the calculated effective magnetic field $\langle\Omega^2_{\mathrm{eff,W}}\rangle$ with the experiment in Fig. 4 shows, however, the validity of the kp expression up to densities $n_D \leqslant 1 \times 10^{19}$ cm^{-3}, corresponding to a Fermi wave vector $k_F = 0.67$ nm^{-1}, while the deviation for the highest investigated density $n_D = 1.5 \times 10^{19}$ cm^{-3} (Fermi wave vector $k_F = 0.76$ nm^{-1}) could originate from an overestimation of the spin splitting by kp theory for large k.[30]

In conclusion, we have investigated the doping density dependence of electron spin relaxation in n-type bulk wurtzite GaN. The spin relaxation time shows a nonmonotonic dependence on the doping density, where the maximum spin lifetime shifts to higher densities for increasing temperature. The decrease of spin lifetimes follows a $\tau_s \propto n_D^{-2/3}$ density dependence in the degenerate regime as a direct consequence of a k-linear spin splitting. The density dependence is described quantitatively without any fitting parameter by an analytical expression for the spin relaxation tensor, as is shown by the determination of both spin relaxation times and momentum scattering times.

We gratefully acknowledge financial support by the German Science Foundation (DFG priority program 1285 "Semiconductor Spintronics") and the German-French University Saarbrücken DFH/UFA (Grant No. CDFA-05-06). J.H.B. and S.S. were supported by the Ruhr-University Research School funded by Germany's Excellence Initiative (Grant No. DFG GSC 98/1).

[1]M. I. Dyakonov and V. I. Perel, Sov. Phys. Solid State **13**, 3023 (1972).
[2]S. Döhrmann, D. Hägele, J. Rudolph, M. Bichler, D. Schuh, and M. Oestreich, Phys. Rev. Lett. **93**, 147405 (2004); O. D. D. Couto, Jr., F. Iikawa, J. Rudolph, R. Hey, and P. V. Santos, *ibid.* **98**, 036603 (2007).
[3]J. H. Jiang and M. W. Wu, Phys. Rev. B **79**, 125206 (2009).
[4]M. Krauß, H. C. Schneider, R. Bratschitsch, Z. Chen, and S. T. Cundiff, Phys. Rev. B **81**, 035213 (2010).
[5]R. I. Dzhioev, K. V. Kavokin, V. L. Korenev, M. V. Lazarev, B. Y. Meltser, M. N. Stepanova, B. P. Zakharchenya, D. Gammon, and D. S. Katzer, Phys. Rev. B **66**, 245204 (2002).
[6]D. Sprinzl, P. Horodyská, N. Tesařová, E. Rozkotová, E. Belas, R. Grill, P. Malý, and P. Němec, Phys. Rev. B **82**, 153201 (2010).
[7]M. W. Wu, J. H. Jiang, and M. Q. Weng, Phys. Rep. **493**, 61 (2010).
[8]B. Beschoten, E. Johnston-Halperin, D. K. Young, M. Poggio, J. E. Grimaldi, S. Keller, S. P. DenBaars, U. K. Mishra, E. L. Hu, and D. D. Awschalom, Phys. Rev. B **63**, 121202(R) (2001).
[9]J. H. Buß, J. Rudolph, F. Natali, F. Semond, and D. Hägele, Appl. Phys. Lett. **95**, 192107 (2009).
[10]J. H. Buß, J. Rudolph, F. Natali, F. Semond, and D. Hägele, Phys. Rev. B **81**, 155216 (2010).
[11]F. Semond, Y. Cordier, N. Grandjean, F. Natali, B. Damilano, S. Vézian, and J. Massies, Phys. Status Solidi A **188**, 501 (2001).
[12]Nonintentionally doped GaN standard template grown by metal-organic chemical vapor deposition by Lumilog, France.
[13]J. H. Buß, J. Rudolph, T. Schupp, D. J. As, K. Lischka, and D. Hägele, Appl. Phys. Lett. **97**, 062101 (2010).
[14]The higher density n_{exc} at $T = 293$ K was used for an improved signal-to-noise ratio. We checked that the spin relaxation times did not change for the increased n_{exc}.
[15]τ_c is a carrier decay time that accounts for a fast initial decay of the TRKR signal due to the decay of the optically excited carrier density. Time-resolved reflectivity measurements gave $\tau_c \approx 10$ ps.
[16]From the dependence $\omega_L(B_{\mathrm{ext}})$ we obtained a Landé g factor of $g = 1.95 \pm 0.02$ for all doping densities, in good agreement with literature values for the electron Landé g factor (Ref. 31).
[17]W. Weber, S. D. Ganichev, S. N. Danilov, D. Weiss, W. Prettl, Z. D. Kvon, V. V. Bel'kov, L. E. Golub, H.-I. Cho, and J.-H. Lee, Appl. Phys. Lett. **87**, 262106 (2005).
[18]J. Y. Fu and M. W. Wu, J. Appl. Phys. **104**, 093712 (2008).
[19]D. Hägele, S. Döhrmann, J. Rudolph, and M. Oestreich, Adv. Solid State Phys. **45**, 253 (2005).
[20]Scattering of electrons with longitudinal optical (LO) phonons can be neglected here because of the large LO phonon energy of 92 meV (Ref. 32).
[21]D. Chattopadhyay and H. J. Queisser, Rev. Mod. Phys. **53**, 745 (1981).
[22]I. Zutic, J. Fabian, and S. D. Sarma, Rev. Mod. Phys. **76**, 323 (2004).
[23]$m^* = 0.2m_e$ is used (Ref. 33).
[24]The extra term due to the interference of WSIA and the Dresselhaus term (see Ref. 10) is negligibly small here.
[25]Indium dots were soldered to the samples as ohmic contacts for the van der Pauw measurements. The momentum scattering time τ_p was determined from $\tau_p = (m^*/e)\mu$, where the mobility $\mu = 1/(en_D\rho)$ was obtained from the known doping density n_D and the resistivity ρ measured by the van der Pauw measurements.
[26]H. M. Ng, D. Doppalapudi, T. D. Moustakas, N. G. Weimann, and L. F. Eastman, Appl. Phys. Lett. **73**, 821 (1998).
[27]J. A. Majewski and P. Vogl, in *Physics of Semiconductors: 27th International Conference on the Physics of Semiconductors*, edited by J. Menéndez and C. G. Van de Walle (AIP, New York, 2005), p. 1403.
[28]M. Cardona, N. E. Christensen, and G. Fasol, Phys. Rev. B **38**, 1806 (1988).
[29]J.-W. Luo, G. Bester, and A. Zunger, Phys. Rev. Lett. **102**, 056405 (2009).
[30]Fu and Wu find a corresponding steep decrease of the Dresselhaus coefficient γ_e for wave vectors $k > 0.7$ nm^{-1} (Ref. 18).
[31]W. E. Carlos, J. A. Freitas, Jr., M. A. Khan, D. T. Olson, and J. N. Kuznia, Phys. Rev. B **48**, 17878 (1993).
[32]J. D. Albrecht, R. P. Wang, P. P. Ruden, M. Farahmand, and K. F. Brennan, J. Appl. Phys. **83**, 4777 (1998).
[33]I. Vurgaftman and J. R. Meyer, J. Appl. Phys. **94**, 3675 (2003).